

# Relaxation functions and dynamical heterogeneities in a model of chemical gel interfering with glass transition

Antonio de Candia<sup>1,2,3,a</sup>, Annalisa Fierro<sup>2</sup>, Raffaele Pastore<sup>2,4</sup>,  
Massimo Pica Ciamarra<sup>2,5</sup> and Antonio Coniglio<sup>1,2</sup>

<sup>1</sup> Dipartimento di Fisica, “Ettore Pancini”, Università di Napoli “Federico II”, Complesso Universitario di Monte Sant’Angelo, via Cintia, 80126 Napoli, Italy

<sup>2</sup> CNR-SPIN, via Cintia, 80126 Napoli, Italy

<sup>3</sup> INFN, Sezione di Napoli, via Cintia, 80126 Napoli, Italy

<sup>4</sup> UC Simulation Center, University of Cincinnati, and Procter & Gamble Co., Cincinnati, Ohio 45219, USA

<sup>5</sup> Division of Physics and Applied Physics, School of Physical and Mathematical Sciences, Nanyang Technological University, Singapore 637371, Singapore

Received 7 June 2016 / Received in final form 26 August 2016

Published online 6 March 2017

**Abstract.** We investigate the heterogeneous dynamics in a model, where chemical gelation and glass transition interplay, focusing on the dynamical susceptibility. Two independent mechanisms give rise to the correlations, which are manifested in the dynamical susceptibility: one is related to the presence of permanent clusters, while the other is due to the increase of particle crowding as the glass transition is approached. The superposition of these two mechanisms originates a variety of different behaviours. We show that these two mechanisms can be unentangled considering the wave vector dependence of the dynamical susceptibility.

## 1 Introduction

Gels and glasses are both amorphous solids. Gels are elastic disordered solids observed at low density in systems of molecules bonded to each other through attractive forces or chemical links. In chemical gels, the transition from sol to gel has been explained [1, 2] in terms of the appearance of a percolating cluster of monomers linked by bonds, that arrests the dynamics in the limit of small wave-vector,  $k_{min} = 2\pi/L$ , with  $L$  being the system size. Experimental measurements have confirmed this geometrical interpretation. Indeed, the chemical sol-gel transition shows the same continuous nature of the random percolation transition. Recently, it has been shown that the same cluster mechanism holds generally for gelling systems [3] and Mode Coupling Theory (MCT) schematic model A [4]. In particular, in references [5, 6] scaling predictions for the time correlation function were obtained, and successfully tested in the  $F_{12}$  MCT

<sup>a</sup> e-mail: [antonio.decandia@unina.it](mailto:antonio.decandia@unina.it)

schematic model and facilitated spin systems on Bethe lattice. Unlike gels, glasses usually exhibit a structural arrest at high density, with the glass transition occurring also in systems of particles only interacting with excluded volume. In this case, the dynamic arrest occurs at all wave-vectors ranging from  $k_{min}$  to  $k_{max} = 2\pi/\sigma$ , where  $\sigma$  is the particle size. Moreover, the glass transition has been associated to an ideal mixed order transition, where a discontinuous order parameter is accompanied by a diverging response, while MCT [4, 7, 8] well describes dynamical behaviour of glassy systems (if not in the deeply supercooled regime).

Despite these fundamental differences, it is not always easy to distinguish between gels and glasses. To this aim it is useful to consider the presence of Dynamic Heterogeneities (DHs), groups of particles dynamically correlated over a time scale of the order of the relaxation time. In particular, the Dynamic Susceptibility  $\chi_4(k, t)$ , commonly used to measure DHs, shows a different behaviour on approaching the two transitions [9]. For chemical gels, it was theoretically shown and numerically verified that at small wave vector (i.e.  $k \rightarrow 0$ ) and long time (i.e.  $t \rightarrow \infty$ ),  $\chi_4(k, t)$  tends to the mean cluster size, which diverges at the gelation threshold with the exponent  $\gamma$  of the random percolation [10, 11]. Indeed, in chemical gels, DHs have a clear static origin. This is different from what occurs in glassy systems, where the dynamical susceptibility displays a maximum in time, whose value increases as the glass transition is approached [12–18]. However, the distinction between gels and glasses may be still elusive when the two transitions coexist, as in some polymer or colloidal systems, where a crossover from gel-like to glass-like behaviour is observed on varying the control parameters (see, for instance, the *PL64/D<sub>2</sub>O AHS* micellar system studied in [19–21]). In this case, the relaxation functions may exhibit complex decays, such as multi-step and logarithmic decays [22–24].

In this paper, we consider a model for polymer suspensions, where the gel and the glass transitions interplay, and investigate the behaviour of the dynamical susceptibility for different wave vectors. We show that  $\chi_4(k, t)$  has a complex behaviour, but that the analysis of the dependence on the wave vector allows to isolate the gel-like features and the glassy-like ones. The gel-like behaviour dominates at small wave vectors, the glassy-like behaviour at large ones, and finally, the combined effect of both transitions at intermediate ones, in analogy with results for models of colloidal gel [25]. We also discuss the dependence of the self Intermediate Scattering Function, on the wave vectors, and the connection with static structure of the system.

## 2 Methods

We consider the same model investigated in Ref. [24]: a 50:50 binary mixture of  $N = 10^3$  hard spheres (monomers) of mass  $m$  and diameters  $\sigma$  and  $1.4\sigma$ , in a box of size  $L$  with periodic boundary conditions. The volume fraction  $\phi = Nv/L^3$ , where  $v$  is the average particle volume, is tuned by changing the size  $L$  of the box. The mass  $m$ , the diameter  $\sigma$  of the smaller particles, and the temperature  $T$ , fix mass, length and energy scales, while the time unit is  $\sqrt{m\sigma^2/T}$ . The wave vector is expressed in unit  $1/\sigma$  (in the following, we fix  $\sigma = 1$ ).

The model is studied using event driven molecular dynamics simulations [26, 27]. After thermal equilibration at the desired volume fraction, permanent bonds are introduced with probability  $p$  between any pair of particles separated by less than  $1.5\sigma$ . A bond corresponds to an infinite square well potential, extending from  $\sigma$  to  $1.5\sigma$ . The procedure used to insert the bonds mimics a light-induced polymerization process, as the number of bonds depends on both  $p$  and  $\phi$ . Here, we consider bond probability 0.4 and different values of the volume fraction. For each set of parameters, we simulate 30–50 realisations of the system with different bond configurations. In refer-

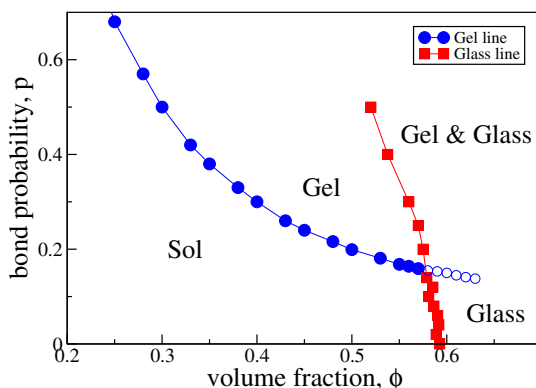


**Fig. 1.** Structural arrest diagram as a function of the volume fraction,  $\phi$ , and of the bonding probability,  $p$ , illustrating the interplay of the gel and the glass transition lines. The gel line is determined via percolative analysis, after introducing bonds with probability  $p$  in an equilibrium (full symbols) or in an out-of-equilibrium (open symbols) monomer suspension. The glass line is defined as that where the extrapolated diffusion coefficient vanishes. Solid lines are guides to the eye (from Ref. [24]).

ences [22, 23] a similar model, in which the bond lifetime may be suitably modulated, has been extensively studied.

### 3 Results

#### 3.1 Phase diagram

We start by reviewing the phase diagram of the investigated model, where the gel is characterised by the presence of a percolating cluster, and the sol-gel transition is identified with the percolation line [24], following references [1, 2]. A standard finite-size scaling analysis of the mean cluster size [28] is applied to identify the percolation line,  $p_{gel}(\phi)$ , i.e. the dependence of the critical value of the bond probability on the volume fraction. As illustrated in Figure 1, it is found that  $p_{gel}(\phi)$  decreases as  $\phi$  increases.

The mean squared displacement is evaluated, and it has been observed that the diffusion coefficient at given bond probability,  $p$ , decreases as a power law  $|\phi - \phi_{glass}|^c$ , approaching a critical value of the volume fraction,  $\phi_{glass}(p)$ , depending on  $p$ . This allowed to identify the glass transition line,  $\phi_{glass}(p)$ , also illustrated in Figure 1. Remarkably, the phase diagram shown in Figure 1 is akin to that obtained in the MCT [4, 7, 8]  $F_{13}$  model [29], with the gel line corresponding to the continuous transition line of the MCT [5, 6] and the glassy line to the discontinuous one. These two lines intersect, the glassy line entering in the gel region, where the liquid-glass transition becomes a gel-glass transition. In the MCT  $F_{13}$  model, the discontinuous transition ends on a high order critical point ( $A_3$  singularity) [4, 30] characterised by logarithm decay of the relaxation functions. Due to long relaxation time involved, it is rather difficult to localise such singularity. However, evidence of logarithmic decay is found [24] in a region inside the gel phase, close to the glass transition line.

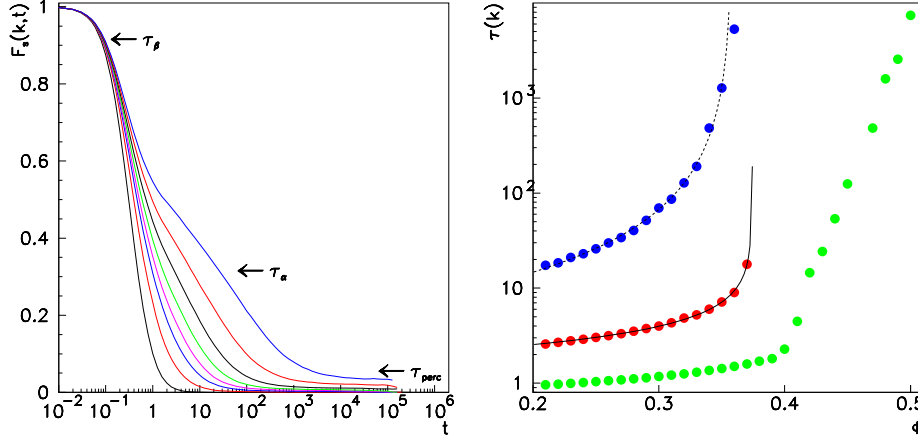


**Fig. 2.** (a) Self ISF,  $F_s(k, t)$  for  $p = 0.4$  and  $k = 6.28$  at different volume fraction  $\phi = 0.4, 0.45, 0.47, 0.48, 0.49, 0.5, 0.51, 0.52$  (from left to right). (b) Relaxation time,  $\tau(k)$ , for  $p = 0.4$  and  $k = 1$  (blue circles),  $k = 3$  (red circles),  $6.28$  (green circles), as function of the volume fraction  $\phi$ . Lines in figure are power law fitting functions,  $A(\phi_f - \phi)^{-\gamma}$ , with and  $A = 0.89$ ,  $\phi_f = 0.36$  and  $\gamma = 1.52$  (dotted line) for  $k = 1$ , and  $A = 1.02$ ,  $\phi_f = 0.37$  and  $\gamma = 0.52$  (continuous line) for  $k = 3$ .

### 3.2 Self intermediate scattering function and dynamical susceptibility

In order to connect the static structure to the dynamical behaviour, we evaluate the self Intermediate Scattering Function (sISF),  $F_s(k, t)$ , and the dynamical susceptibility,  $\chi_4(k, t)$ , defined respectively as:

$$F_s(k, t) = [\langle \Phi_s(k, t) \rangle], \quad (1)$$

$$\chi_4(k, t) = N [\langle |\Phi_s(k, t)|^2 \rangle - \langle \Phi_s(k, t) \rangle^2], \quad (2)$$

where  $\Phi_s(k, t) = \frac{1}{N} \sum_{i=1}^N e^{i\mathbf{k} \cdot (\mathbf{r}_i(t) - \mathbf{r}_i(0))}$ ,  $\langle \dots \rangle$  is the thermal average,  $[\dots]$  is the average over the bond configurations, and the sums are done on all particles.

Three different relaxation time scales are recognised [24] in the relaxation functions:  $\tau_\beta$ , due to the rattling of particles in cage formed by the neighbors [31–33];  $\tau_\alpha > \tau_\beta$ , due to the opening of the cage, diverging at the glass transition line; and finally  $\tau_{perc} > \tau_\alpha$ , due to the relaxation of the largest cluster, diverging at the gel transition line (see Fig. 2a). Similar findings are obtained in references [22, 23]. At  $\phi > \phi_{gel}$ ,  $F_s(k, t)$ , does not relax to zero, and reaches at long time a finite value, due to particles belonging to the spanning cluster, that decreases as the wave vector  $k$  increases, and increases as a function of the volume fraction. Thus, evaluating the integral relaxation time,  $\tau(k) \equiv \int dt t F_s(k, t) / \int dt F_s(k, t)$ , we expect  $\tau(k)$  to diverge at the percolation transition

In Figure 2b,  $\tau(k)$  is plotted as function of the volume fraction for different wave vectors. We observe a divergence of  $\tau(k)$  for  $k = 1$  and  $k = 3$  roughly at the percolation threshold,  $\phi_c \sim 0.37$ , obtained from the divergence of the mean cluster size, whereas  $\tau(k)$  for  $k = 6.28$  smoothly increases for  $\phi > \phi_{gel}$ . We suggest that the behaviour of the relaxation time, at  $k = 6.28$ , is a numerical artifact: at large wave vectors and small volume fraction, due to the numerical accuracy reachable in the simulations, the plateau, reached at long time, is so small that it is not observable at

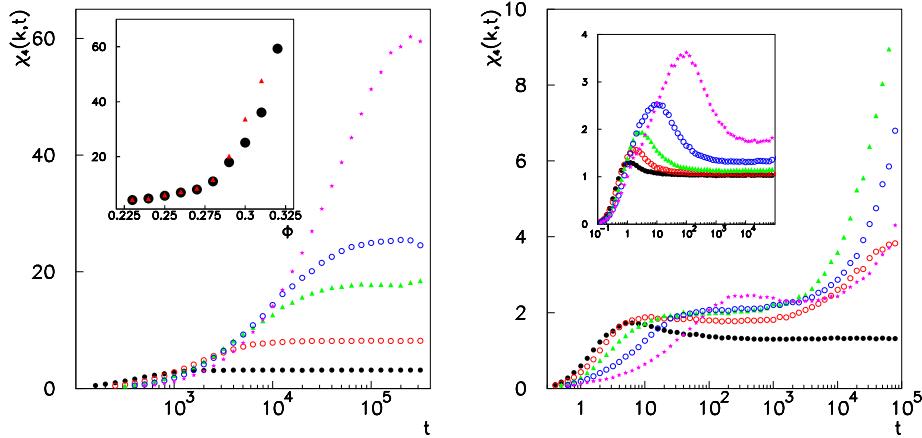


**Fig. 3.** (a) **Main frame:** Dynamical susceptibility,  $\chi_4(k, t)$ , for  $p = 0.4$ ,  $k = 0.1$  and  $\phi = 0.21, 0.27, 0.29, 0.3, 0.32$  (from bottom to top). **Inset:** Asymptotic value of the dynamical susceptibility (black circles) and mean cluster size of the large particles (red triangles). (b) **Main frame:** Dynamical susceptibility,  $\chi_4(k, t)$ , for  $p = 0.4$ ,  $k = 3$  and  $\phi = 0.4, 0.44, 0.47, 0.5, 0.52$  (same symbols as in the inset). **Inset:** Dynamical susceptibility  $\chi_4(k, t)$  for  $p = 0.4$ ,  $k = 6.28$  and  $\phi = 0.4, 0.44, 0.47, 0.5, 0.52$  (from bottom to top).

all in our data (see Fig. 2a), and apparently it seems that the relaxation time is finite also in the gel phase.

So, the percolating cluster dominates the self ISF long time decay. Conversely, as it has been also observed in reference [24], finite clusters dominate the long time mean square displacement, which results to be diffusive also in the gel phase, with a diffusion coefficient vanishing only at the glass transition line.

In references [10,11], the gel formation is studied in a model system undergoing a chemical gelation by means of molecular dynamics simulations. Approaching the gelation threshold from the sol phase, the dynamic susceptibility is found to be a monotonic function increasing with time, which tends in the limit of long times to a plateau, whose value diverges, as a function of the distance from the gelation transition, as the mean cluster size. Moreover, it has been theoretically shown that, in general in chemical gels, in the thermodynamics limit, at small enough wave vectors  $k$ , such as  $2\pi/k > \xi$  with  $\xi$  the average linear size of the largest cluster, the dynamic susceptibility obtained from the self ISF actually tends to the mean cluster size. In the following, we will check this prediction in the model here studied. In Figure 3a, the dynamical susceptibility,  $\chi_4(k, t)$ , is plotted for  $k = 0.1$  (for wave vector  $k < 0.1$ , the relaxation time becomes extremely long and we observe only the transient behaviour of the dynamical susceptibility). Indeed, we observe that  $\chi_4(k, t)$  tends to a plateau (see main frame of Fig. 3a) that coincides with the mean cluster size at small volume fraction (see inset of Fig. 3a). A deviation is observed approaching the percolation threshold, where  $\xi$  diverges and the condition  $2\pi/k > \xi$  does not hold yet. At the largest wave vector ( $k = 6.28$ ), due to the crowding of particles,  $\chi_4(k, t)$  displays a maximum, as usually observed in glassy systems, whose value increases as the glass transition is approached (see inset of Fig. 3b), and, due to the presence of permanent clusters, a plateau different from 1 at long times. At intermediate wave vector ( $k = 3$ ), the superposition of these two mechanisms gives origin to more complex features, as we can see in main frame of Figure 3b.

## 4 Discussion

The presence of permanent bonds in gelling system generates correlation between the positions of pairs of particles belonging to the same cluster, which manifests as a plateau in the dynamical susceptibility. Interestingly this type of behaviour is very similar to that observed in a spin glass model [34], and it is the signal that heterogeneities in chemical gel have a static nature. In the limit of small wave vector, this plateau coincides with the mean cluster size and diverges at the gelation threshold. In systems, where both glass and gel transitions are present, a second mechanism, due to the crowding, contributes to the dynamical susceptibility, as correlation between the displacements of different particles. Here, we have clarified that these two mechanisms can be unentangled considering the wave vector dependence of the dynamical susceptibility. The superposition of these two mechanisms originates a range of different behaviours, depending on the wave vector.

Finally we would like to dedicate this paper to Professor Alberto Robledo for his great scientific achievements on the occasion of his 70<sup>th</sup> Birthday.

We acknowledge financial support from MIUR-FIRB RBF081IUK, from the SPIN SEED 2014 project *Charge separation and charge transport in hybrid solar cells*, and from the CNR-NTU joint laboratory *Amorphous materials for energy harvesting applications*.

## References

1. P.J. Flory *Principles of Polymer Chemistry* (Cornell University Press, Ithaca, NY, 1954)
2. P.G. de Gennes *Scaling Concepts in Polymer Physics* (Cornell University Press, Ithaca, NY, 1993)
3. A. Fierro, T. Abete, A. Coniglio, J. Chem. Phys. **131**, 194906 (2009)
4. W. Götze, J. Phys.: Condens. Matter **11**, A1 (1999)
5. J.J. Arenzon, A. Coniglio, A. Fierro, M. Sellitto, Phys. Rev. E **90**, 020301(R) (2014)
6. A. Coniglio, J.J. Arenzon, A. Fierro, M. Sellitto, Eur. Phys. J. Special Topics **223**, 2297 (2014)
7. W. Götze *Complex dynamics of glass-forming liquids*, (Oxford University Press, Oxford, 2009)
8. W. Götze, L. Sjogren, Rep. Prog. Phys. **55**, 241 (1992)
9. R. Pastore, A. de Candia, A. Fierro, M. Pica Ciamarra, A. Coniglio, J. Stat. Mech. **2016**, 074011 (2016)
10. T. Abete, A. de Candia, E. Del Gado, A. Fierro, A. Coniglio, Phys. Rev. Lett. **98**, 088301 (2007)
11. T. Abete, A. de Candia, E. Del Gado, A. Fierro, A. Coniglio, Phys. Rev. E **78**, 041404 (2008)
12. W. Kob, C. Donati, S.J. Plimpton, P.H. Poole, S.C. Glotzer, Phys. Rev. Lett. **79**, 2827 (1997)
13. S. Franz, G. Parisi, J. Phys.: Condens. Matter **12**, 6335 (2000)
14. L. Berthier et al., Science **310**, 1797 (2005)
15. G. Biroli, J.P. Bouchaud, K. Miyazaki, D.R. Reichman, Phys. Rev. Lett. **97**, 195701 (2006)
16. L. Berthier et al., J. Chem. Phys. **126**, 184503 (2007)
17. C. Dalle-Ferrier et al., Phys. Rev. E **76**, 041510 (2007)
18. R. Pastore, M. Pica Ciamarra, A. Coniglio, Fractals **21**, 1350021 (2013)
19. F. Mallamace, S.H. Chen, A. Coniglio, L. de Arcangelis, E. Del Gado, A. Fierro, Phys. Rev. E **73**, 020402 (2006)
20. S.H. Chen, W.R. Chen, F. Mallamace, Science **300**, 619 (2003)
21. F. Mallamace, C. Corsaro, H.E. Stanley, D. Mallamace, S.H. Chen, J. Chem. Phys. **139**, 214502 (2013)

22. P. Chaudhuri, P.I. Hurtado, L. Berthier, W. Kob, *J. Chem. Phys.* **142**, 174503 (2015)
23. P. Chaudhuri, L. Berthier, P.I. Hurtado, W. Kob, *Phys. Rev. E* **81**, 040502 (2010)
24. N. Khalil, A. de Candia, A. Fierro, M. Pica Ciamarra, A. Coniglio, *Soft Matter* **10**, 4800 (2014)
25. A. de Candia, E. Del Gado, A. Fierro, A. Coniglio, *J. Stat. Mech.* **2009**, P02052 (2009)
26. B.D. Lubachevsky, *J. Comput. Phys.* **94**, 255 (1991)
27. M.P. Allen, D.J. Tildesley, *Computer Simulation of Liquids* (Oxford University Press, Oxford, 1987)
28. D. Stauffer, A. Aharony, *Introduction to percolation theory* (Taylor & Francis, London, 1992)
29. W. Götze, M. Sperl, *Phys. Rev. E* **66**, 011405 (2002)
30. K. Dawson, M. Foffi, M. Fuchs, W. Götze, F. Sciortino, M. Sperl, P. Tartaglia, T. Voigtmann, E. Zaccarelli, *Phys. Rev. E* **63**, 011401 (2000)
31. M. Pica Ciamarra, R. Pastore, A. Coniglio, *Soft Matter* **12**, 358 (2016)
32. R. Pastore, A. de Candia, A. Fierro, A. Coniglio, M. Pica Ciamarra, *J. Stat. Mech.* **2016**, 054050 (2016)
33. R. Pastore, A. Coniglio, M. Pica Ciamarra, *Soft Matter* **11**, 7214 (2015)
34. A. Fierro, A. de Candia, A. Coniglio, *Phys. Rev. E* **62**, 7715 (2000)